Available online at www.sciencedirect.com
SCIENCE DIRECT®
Journal of Solid State Chemistry 177 (2004) 1681–1694
JOURNAL OF SOLID STATE CHEMISTRY
http://elsevier.com/locate/jssc

Two new lithium uranyl tungstates $Li_2(UO_2)(WO_4)_2$ and $Li_2(UO_2)_4(WO_4)_4O$ with framework based on the uranophane sheet anion topology

S. Obbade,* S. Yagoubi, C. Dion, M. Saadi,[1] and F. Abraham

Laboratoire de Cristallochimie et Physicochimie du Solide, CNRS UMR 8012, ENSCL-USTL, BP 108, 59652 Villeneuve d'Ascq cedex, France

Received 23 October 2003; received in revised form 15 December 2003; accepted 18 December 2003

Abstract

Two new lithium uranyl tangstates $Li_2(UO_2)(WO_4)_2$ and $Li_2(UO_2)_4(WO_4)_4O$ have been prepared by high-temperature solid state reactions of Li_2CO_3, U_3O_8 and WO_3. For each compound, the crystal structure was determined by single crystal X-ray diffraction data, using a Brucker diffractometer, equipped with a SMART CCD detector and Mo$K\alpha$ radiation. The crystal structures were solved at room temperature by direct methods followed by Fourier difference techniques, and refined by a least square procedure on the basis of F^2 for all independent reflections, to $R_1 = 0.035$ for 65 refined parameters and 807 reflections with $I \geqslant 2\sigma(I)$ for $Li_2(UO_2)(WO_4)_2$ and to $R_1 = 0.051$ for 153 refined parameters and 1766 reflections with $I \geqslant 2\sigma(I)$ for $Li_2(UO_2)_4(WO_4)_4O$.

The crystal structure of $Li_2(UO_2)(WO_4)_2$ is formed by perovskite sheets of WO_6 octahedra, one octahedron thickness, connected together by $(UO_5)_\infty$ infinite chains, and creating tunnels parallel to the c-axis. The lithium atoms are localized in the tunnels. The structure can be deduced from that of UMO_5 (M = Mo, V, Nb) compounds by the replacement of half U atoms by Li. The crystal structure of $Li_2(UO_2)_4(WO_4)_4O$ consists of UO_7 pentagonal bipyramids, UO_6 tetragonal bipyramids and WO_6 distorted octahedra linked together to form a three-dimensional framework creating paralleled channels filled with lithium cations. The structure can also be described by the stacking of layers with the uranophane sheet anion topology similar to those obtained in UMO_5 (M = Mo, V, Nb, Sb) compounds with an ordered population of pentagons by U and Li and of squares by U and W. The measured conductivities are comparable to those of the better Li^+ ion conductor solid electrolytes such as LISICON or Li-β-alumina.

Crystallographic data: $Li_2(UO_2)(WO_4)_2$, orthorhombic symmetry, space group *Pbcn* and unit cell parameters $a = 7.9372(15)$ Å, $b = 12.786(2)$ Å, $c = 7.4249(14)$ Å, $\rho_{cal} = 6.87(2)$ g/cm^3, $\rho_{mes} = 6.89(1)$ g/cm^3 and $Z = 4$. $Li_2(UO_2)_4(WO_4)_4O$, monoclinic symmetry, space group $C2/c$ and unit cell parameters $a = 14.019(4)$ Å, $b = 6.3116(17)$ Å, $c = 22.296(6)$ Å, $\beta = 98.86(3)^\circ$, $\rho_{cal} = 7.16(2)$ g/cm^3, $\rho_{mes} = 7.25(3)$ g/cm^3 and $Z = 4$.

Keywords: Alkali uranyl tungstates; Crystal structure refinement; Solid state synthesis; Cationic conductivity

1. Introduction

Uranyl molybdates have received considerable attention these last years because, independently of the mineralogical and environmental aspects, they present an important structural interest if we consider the Mo^{6+} coordination possibilities leading to different oxoanions with tetrahedral, square pyramidal or octahedral environment. This structural wealth can be illustrated by the following examples of different monovalent ion uranyl molybdates.

Mostly, Molybdenum atom is tetrahedrally coordinated by O atoms, this is particularly right for numerous compounds based on the binary lines UO_2MoO_4–M_2MoO_4 and formulated $M_2(UO_2)_6(MoO_4)_7{\cdot}H_2O$ ($M = NH_4$, Cs) [1,2], $(NH_4)_4[(UO_2)_5(MoO_4)_7](H_2O)_5$ [3], $Cs_2(UO_2)_2(MoO_4)_3$ [4], $M_2UO_2(MoO_4)_2$ with M =

*Corresponding author. Fax: +33-320436814.
E-mail address: obbade@ensc-lille.fr (S. Obbade).
[1] Laboratoire de Chimie de Coordination et Analytique, Faculté des Sciences, Université Chouaib Doukkali, B.P. 20, El Jadida, Maroc.

0022-4596/$ - see front matter © 2004 Elsevier Inc. All rights reserved.
doi:10.1016/j.jssc.2003.12.029

Na, K, Rb [5–7], $M_6UO_2(MoO_4)_4$ with M = Na, K and Cs [8,9]. Tetrahedral MoO_4 oxoanions are also found in the recently studied $K_2(UO_2)_2(MoO_4)O_2$ compound [10]. Square pyramid coordination is more uncommon but has been observed in $K_8(UO_2)_8(MoO_5)_3O_6$ [10]. To our knowledge, no example of uranyl-alkali metal molybdates with Mo^{6+} in octahedral environment has been published up today, but this coordination exists in the structure of UMo_2O_8 [11], and hydrated mineralogical varieties such umohoïte $[(UO_2)MoO_4(H_2O)]H_2O$ [12], iriginite $UO_2Mo_2O_7 \cdot 2H_2O$ [13,14] and several alkali molybdates, $M_2Mo_2O_7$ (M = Na, K) [15,16] or $K_2Mo_4O_{13}$ [17].

These alkali metal uranyl compounds present mostly layered structures which confer to them potential properties in the domains of intercalation, ionic exchange and electrical ionic conductivity due to the interlayers cations mobility. In some cases like $M_2(UO_2)_6(MoO_4)_7 \cdot H_2O$ [1,2], a three-dimensional framework is observed.

The same diversity of polyhedra and analogous compounds are expected for W^{6+}. For example, anhydrous uranyl oxides of the family UO_2XO_4 with X = S, Cr, Se, Mo and W are well known [18–21] and adopt the same crystal structure which results from the association of $(UO_2)O_5$ pentagonal bipyramids sharing four equatorial oxygen atoms with different XO_4 tetrahedra, the last equatorial oxygen atom being shared with an apical oxygen atom of a neighboring $(UO_2)O_5$ bipyramid. During the study of the UO_2–WO_3 system, four phases $U(WO_4)_2$, UW_3O_{11}, UW_4O_{14} and UW_5O_{17} have been identified by X-ray powder diffraction and high resolution electron microscopy [22]. The first compound is isotypic to the orthorhombic $Th(MoO_4)_2$ [23] with eight-coordinated uranium and four-coordinated tungsten. The other compounds are related to orthorhombic UMo_2O_8 [11], the structures are built from the intergrowth of corner-sharing WO_6 octahedra in ReO_3-type slabs of different thickness with slabs of edge-sharing UO_7 pentagonal bipyramids. Finally, another uranyl tungstate $UO_2(W_3O_{10})$ [24] is reported but its structure is unknown. The only indication of alkali metal uranyl tungstate found in the literature is about the preparation of $Na_2UO_2(WO_4)_2$ compound [25], but without any crystal structure characterization.

Recent studies in our group have focused on the preparation of new uranyl tungstates with various crystal structures. These efforts have resulted in the preparation of new alkali metal uranyl tungstates that belong to three families, $M_2UO_2(W_2O_8)$ with M = Na, K, $M_2(UO_2)_2(WO_5)O$ with M = K, Rb and $Na_{10}(UO_2)_8(W_5O_{20})O_8$ [26] where the tungsten atoms in the highest possible oxidation state adopt the three possible coordinations, tetrahedral, square pyramidal and octahedral. In the first family one-dimensional chains formed from edge-sharing UO_7 pentagonal bipyramids are connected by two octahedra wide $(W_2O_8)_\infty$ ribbons formed from two edge-sharing WO_6 octahedra connected together by corners to built $[(UO_2(W_2O_8)^{2-}]_\infty$ infinite layers. In the second family $M_2(UO_2)_2(WO_5)O$ (M = K, Rb), the coordination polyhedron of W^{6+} is a square pyramid and in $Na_{10}(UO_2)_8(W_5O_{20})O_8$, W^{6+} is both in tetrahedral and octahedral coordination to give W_5O_{20} units resulting from a WO_4 tetrahedron shares corners to four WO_6 octahedra. Very recently, the first family has been enriched with the crystal structure report of $Na_2UO_2(W_2O_8)$ and α and β forms of $Ag_2UO_2(W_2O_8)$ [27].

It is interesting to remark that the structural isotypy between molybdenum and tungsten compounds in the UO_2XO_4 family (X = S, Cr, Se, Mo, W), is generally not observed in doubled compounds of uranyl and alkali metals. For example, the compounds $K_2UMo_2O_{10}$ and $K_2UW_2O_{10}$ do not adopt the same crystal structure and their formulae must be written $K_2UO_2(MoO_4)_2$ [6] and $K_2UO_2(W_2O_8)$ [26], respectively, because the cation Mo^{6+} is tetrahedrally coordinated whereas W^{6+} atom is in octahedral coordination to give W_2O_8 dimmers. A similar remark is available for $K_2U_2MoO_{10}$ and $K_2U_2WO_{10}$ which can be written $K_2(UO_2)_2(MoO_4)O_2$ [10] and $K_2(UO_2)_2(WO_5)O$ [26], respectively, to differentiate the tetrahedral coordination of Mo^{6+} from the square pyramidal coordination of W^{6+}.

As lithium often presents a particular behavior compared to the other alkali metals, it seemed interesting to study the ternary system Li_2CO_3–U_3O_8–WO_3 to see the effect of lithium on the structure as well as on the conductivity properties. Thus, two new compounds were obtained and the present work is dedicated to the synthesis, and crystal structure determination of two new uranyl–lithium tungstates, $Li_2UW_2O_{10}$ or $[Li_2UO_2(WO_4)_2]$ and $Li_2U_4W_4O_{25}$ or $[Li_2(UO_2)_4(WO_4)_4O]$ presenting original three-dimensional structural arrangements. Conductivity measurements are also reported for both compounds.

2. Experimental

2.1. Crystal and powder synthesis

Single crystals of $Li_2UO_2(WO_4)_2$ and $Li_2(UO_2)_4(WO_4)_4O$ were obtained by solid state reaction. Both compounds were prepared using a mixture of Li_2CO_3 (Aldrich), U_3O_8 (Prolabo) and WO_3 (Prolabo) in the molar ratio 1,2/3,1. The resulting of 2 g charge was thoroughly mixed and heated in a platinum crucible at 920°C during 48 h and slowly cooled at 5°C/h to room temperature. Washing of the obtained yellowish shiny crystalline product with ethanol allowed the separation of two kinds of single crystals. The yellow single crystals correspond to the $Li_2(UO_2)_4(WO_4)_4O$

phase and the orange colored single crystals belong to the $Li_2UO_2(WO_4)_2$ compound.

For both compounds, powder samples were synthesized by a solid state reaction between stoichiometric mixtures of Li_2CO_3, WO_3 and U_3O_8 according to the following reactions:

$$Li_2CO_3 + 2WO_3 + \tfrac{1}{3}U_3O_8 + \tfrac{1}{6}O_2 \rightarrow Li_2UO_2(WO_4)_2 + CO_2 \quad (1)$$

and

$$Li_2CO_3 + 4WO_3 + \tfrac{4}{3}U_3O_8 + \tfrac{2}{3}O_2 \rightarrow Li_2(UO_2)_4(WO_4)_4O + CO_2 \quad (2)$$

Mixed starting materials in the appropriate stoichiometries were heated at high temperature in air for two weeks with intermediate grindings. Pure powder samples were obtained at 600°C and 750°C for $Li_2UO_2(WO_4)_2$ and $Li_2(UO_2)_4(WO_4)_4O$, respectively. The achievement of the synthesis process for each sample was controlled by X-ray powder diffraction using a Guinier-De Wolff focusing camera and Cu$K\alpha$ radiation.

2.2. Single crystal X-ray diffraction and structure determination

Well-shaped crystals of for $Li_2UO_2(WO_4)_2$ and $Li_2(UO_2)_4(WO_4)_4O$, with dimensions 0.080 mm–0.240 mm–0.062 mm and 0.030 mm–0.150 mm–0.052 mm, respectively, were selected for structure determination. Each single crystal was mounted on a Bruker Platform three circle X-ray diffractometer equipped with an 1 K SMART CCD detector and operating at 50 kV and 40 mA. For both compounds, preliminary unit cell parameters were determined from 30 frames with 20 s exposure times. For each crystal, the intensities of reflections for a sphere were measured with a graphite monochromated Mo$K\alpha$ radiation, using a combination of three sets of 600 frames, where each frame covered a range of 0.3° in ω scan. Thus, a total of 1800 frames were collected with an exposure time of 50 s per frame. The intensity reduction and correction of Lorentz, polarization and background effects, were done by the program SAINTPLUS 6.02 [28]. For each single crystal data, absorption corrections based on the precise crystal morphology and indexed crystal faces were applied using the program XPREP of the SHELXTL package [29] followed by SADABS program [30]. Systematic absences of reflections were consistent with *Pbcn* and $C2/c$ centro-symmetric space groups for $Li_2UO_2(WO_4)_2$ and $Li_2(UO_2)_4(WO_4)_4O$, respectively. The crystal structures were solved by a combination of direct methods and difference Fourier syntheses, and refined by full matrix least squares against F^2, using SHELXTL package of programs [29]. Relevant crystallographic information are compiled in Table 1, and the final atomic positions with isotropic (Li) or equivalent (U, W and O atoms) thermal displacements, and anisotropic displacement parameters for U, W and O atoms, are presented in Tables 2 and 3 for $Li_2UO_2(WO_4)_2$, and in Tables 5 and 6 for $Li_2(UO_2)_4(WO_4)_4O$, respectively. Selected interatomic distances with uranyl ion angles, and bond valence sums calculated using Burns et al. data [31] for U–O bonds and Brese and O'Keeffe parameters [32] for the other bonds, are reported in Table 4 and 7 for $Li_2UO_2(WO_4)_2$ and $Li_2(UO_2)_4(WO_4)_4O$, respectively.

2.3. Powder compounds characterization

For each compound, powder X-ray diffraction data used for lattice parameters refinement were recorded on a Siemens D5000 $\theta/2\theta$ diffractometer, at room temperature, using Bragg-Brentano geometry, with a back-monochromatized Cu$K\alpha$ radiation. The diffraction patterns were scanned over the angle range 10–80°(2θ) in step of 0.03°(2θ) and a counting time of 20 s per step. The unit cell parameters were refined by a least-squares procedure from the indexed powder reflections. Powder X-ray diffraction pattern data and refined cell parameters with their merit factors F_{20}, as defined by Smith and Snyder [33], are reported in Tables 8 and 9 for $Li_2UO_2(WO_4)_2$ and $Li_2(UO_2)_4(WO_4)_4O$, respectively.

The densities measured with an automated Micromeritics Accupyc 1330 helium pycnometer using a 1-cm^3 cell, indicated $Z = 4$ formula per unit cell for both compounds, with ($\rho_{mes} = 6.89(1)\,g\,cm^{-3}$, $\rho_{cal} = 6.87(2)\,g\,cm^{-3}$) and ($\rho_{mes} = 7.25(3)\,g\,cm^{-3}$, and $\rho_{cal} = 7.16(2)\,g\,cm^{-3}$) for $Li_2UO_2(WO_4)_2$ and $Li_2(UO_2)_4(WO_4)_4O$, respectively.

For both compounds, differential thermal analysis (DTA) was carried out in air on a Setaram 92–1600 thermal analyzer in the temperature range 20–1100°C both on heating and cooling. These measurements showed the existence of non-congruent melting points for both compounds at about 720°C and 940°C for $Li_2UO_2(WO_4)_2$ and $Li_2(UO_2)_4(WO_4)_4O$, respectively. The decomposition of both compounds was also confirmed by powder X-ray diffraction analyses of residues after each DTA measurement showing the formation of $Li_2U_4W_4O_{25}$ and Li_2WO_4 for $Li_2UO_2(WO_4)_2$, of U_3O_8 and Li_2WO_4 for $Li_2UO_2(WO_4)_2$, accompanied by unidentified phases.

For conductivity measurements, powder samples were pelletized at room temperature and then sintered 50°C below their melting point for 2 h. Gold electrodes were sputtered on both flat faces and measurements were done by impedance spectrometry in the frequency range 1–10^6 Hz with a Schlumberger 1170 frequency response analyzer. Measurements were made at 20°C intervals over the range 200–600°C, on both heating and cooling. Each set of values was recorded at a given temperature after a 1 h stabilization time.

Table 1
Crystal data, intensity collection and structure refinement parameters for $Li_2(UO_2)(WO_4)_2$ and $Li_2(UO_2)_4(WO_4)_4O$.

	$Li_2(UO_2)(WO_4)_2$		$Li_2(UO_2)_4(WO_4)_4O$	
Crystal data				
Crystal symmetry	Orthorhombic		Monoclinic	
Space group	*Pbcn*		*C*2/*c*	
Unit cell refined from	$a = 7.9372(15)$ Å		14.019(4) Å	
Single crystal data	$b = 12.786(2)$ Å		6.3116(17) Å	
	$c = 7.4249(14)$ Å		22.296(6) Å	
			$\beta = 98.86(3)^\circ$	
Unit cell volume	753.52(20) Å^3		1949.2(9) Å^3	
Z	4		4	
Calculated density (g cm^{-3})	$\rho = 6.87(2)$		7.16(2)	
Measured density (g cm^{-3})	$\rho = 6.89(1)$		7.25(3)	
Color	Orange		Yellow	
Data collection				
Temperature (K)	293(2)		293(2)	
Equipment	Bruker SMART CCD		Bruker SMART CCD	
Radiation Mo*K*α	0.71073 Å		0.71073 Å	
Scan mode	ω		ω	
Recording θ min/max (°)	4.08/29.24		2.94/29.99	
Recording reciprocal space	$-10 \leqslant h \leqslant 10$		$-16 \leqslant h \leqslant 19$	
	$-17 \leqslant k \leqslant 17$		$-8 \leqslant k \leqslant 8$	
	$-10 \leqslant l \leqslant 10$		$-30 \leqslant l \leqslant 30$	
No. of measured reflections	4406		5437	
No. of independent reflections	807		1766	
Absorption coefficient μ (cm^{-1})	519.32		567.23	
Limiting faces and distances (mm)	1 0 0	0.040	1 0 0	0.015
From an arbitrary origin	$\bar{1}$ 0 0	0.040	$\bar{1}$ 0 0	0.015
	0 1 0	0.140	0 1 0	0.075
	0 $\bar{1}$ 0	0.140	0 $\bar{1}$ 0	0.075
	0 0 1	0.031	0 0 1	0.026
	0 0 $\bar{1}$	0.031	0 0 $\bar{1}$	0.026
R merging factor	0.034		0.077	
Refinement				
Refined parameters/restraints	65/0		153/0	
Goodness of fit on F^2	1.027		0.996	
R_1 [$I > 2\sigma(I)$]	0.035		0.051	
wR_2 [$I > 2\sigma(I)$]	0.085		0.103	
R_1 for all data	0.037		0.054	
wR_2 for all data	0.088		0.113	
Largest diff. peak and hole(e Å^{-3})	5.292/−4.000		4.690/−5.515	

$R_1 = \sum(|F_o| - |F_c|)/\sum|F_o|$, $wR_2 = [\sum w(F_o^2 - F_c^2)^2/\sum w(F_o^2)^2]^{1/2}$, $w = 1/[\sigma^2(F_o^2) + (aP)^2 + bP]$ where *a* and *b* are refinable parameters and $P = (F_o^2 + 2F_c^2)/3$.

Table 2
Atomic positions, equivalent or isotropic displacement parameters (Å^2) of $Li_2(UO_2)(WO_4)_2$.

Atom	Site	Occ	*x*	*y*	*z*	U_{eq}/U_{iso}*
U	4*c*		0	0.02101(5)	1/4	0.0133(2)
W	8*d*		0.03779(6)	0.25671(3)	0.00005(8)	0.0048(2)
O(1)	8*d*		−0.2277(17)	0.0222(9)	0.257(2)	0.028(3)
O(2)	4*c*		0	0.2122(11)	1/4	0.010(2)
O(3)	4*c*		0	0.2675(11)	3/4	0.013(2)
O(4)	8*d*		0.2563(17)	0.2505(7)	0.0209(19)	0.015(2)
O(5)	8*d*		0.0113(17)	0.3914(7)	0.0436(14)	0.012(2)
O(6)	8*d*		0.005(2)	0.0999(7)	−0.0309(13)	0.015(2)
Li(1)	4*c*	0.67[a]	0	0.491(4)	3/4	0.012(9)*
Li(2)	8*d*	0.67[a]	−0.168(5)	0.496(2)	−0.033(5)	0.014(7)*

[a] Fixed value.

Table 3
Anisotropic displacement parameters for U, W and O of $Li_2(UO_2)(WO_4)_2$ ($Å^2$).

Atom	U_{11}	U_{22}	U_{33}	U_{12}	U_{13}	U_{23}
U	0.0284(4)	0.0086(3)	0.0031(3)	0	0.0001(4)	0
W	0.0051(3)	0.0065(3)	0.0028(3)	−0.0002(1)	0.0001(2)	0.0001(2)
O(1)	0.039(6)	0.014(5)	0.032(7)	−0.001(4)	0.000(8)	−0.016(8)
O(2)	0.008(6)	0.018(7)	0.005(6)	0	0.003(7)	0
O(3)	0.022(7)	0.012(6)	0.006(6)	0	−0.005(9)	0
O(4)	0.020(7)	0.019(5)	0.006(3)	0.000(4)	0.003(5)	0.002(3)
O(5)	0.012(5)	0.007(4)	0.017(5)	−0.004(4)	0.001(5)	−0.002(4)
O(6)	0.034(6)	0.004(4)	0.007(4)	−0.001(5)	−0.006(6)	−0.002(3)

Note: The anisotropic displacement factor exponent takes the form $-2\pi^2[h^2a^{*2}U_{11} + \cdots + 2hka^*b^*U_{12}]$.

Table 4
Bond distances (Å), angles (°) and bond valences S_{ij} of metal atoms in $Li_2(UO_2)(WO_4)_2$.

U environment		
		s_{ij}
U–O(1)^{i}	1.808(13)	1.597
U–O(1)	1.808(13)	1.597
U–O(6)^{ii}	2.245(9)	0.688
U–O(6)^{iii}	2.245(9)	0.688
U–O(6)^{i}	2.317(10)	0.599
U–O(6)	2.317(10)	0.599
U–O(2)	2.445(14)	0.468
O(1)^{i}–U–O(1)	179.1(6)	$\sum s_{ij}$ 6.239
W environment		
		s_{ij}
W–O(4)	1.743(14)	1.600
W–O(5)	1.765(9)	1.512
W–O(3)^{x}	1.886(1)	1.087
W–O(2)^{iv}	1.964(4)	0.881
W–O(6)	2.035(9)	0.727
W–O(4)^{v}	2.242(14)	0.417
O5–W–O(6)	165.2 (4)	$\sum s_{ij}$ 6.224
Li environment		
		s_{ij}
Li1–O(5)^{vi}	2.149(37)	0.157
Li1–O(5)^{vii}	2.149(37)	0.157
Li1–O(1)^{viii}	2.169(14)	0.150
Li1–O(1)^{ix}	2.169(14)	0.150
Li1–O(5)^{x}	2.526(28)	0.057
Li1–O(5)^{i}	2.526(28)	0.057
Li1–O(3)	2.858(20)	0.023
		$\sum s_{ij}$ 0.751
Li2–O(1)^{xi}	1.781(40)	0.428
Li2–O(5)^{xii}	1.904(34)	0.301
Li2–O(5)	2.034(36)	0.218
Li2–O(1)^{xiii}	2.331(40)	0.097
		$\sum s_{ij}$ 1.044

Symmetry codes: (i) $-x, y, 0.5-z$; (ii) $-x, -y, -z$; (iii) $x, -y, 0.5+z$; (iv) $x, y, -1+z$; (v) $-0.5+x, 0.5-y, -z$; (vi) $-x, 1-y, 1-z$; (vii) $x, 1-y, 0.5+z$; (viii) $0.5+x, 0.5-y, 1-z$; (ix) $-0.5-x, 0.5-y, 0.5+z$; (x) $x, y, 1+z$; (xi) $-0.5-x, 0.5-y, -0.5+z$; (xii) $-x, 1-y, -z$; (xiii) $-0.5-x, 0.5+y, z$.

Table 5
Atomic positions, equivalent or isotropic displacement parameters ($Å^2$) of $Li_2(UO_2)_4(WO_4)_4O$.

Atom	Site	x	y	z	$U_{iso}{}^*/U_{eq}$
U(1)	4*e*	0	0.04210(19)	3/4	0.0086(3)
U(2)	4*a*	1/2	1/2	0	0.0095(3)
U(3)	8*f*	0.29366(6)	0.44785(14)	0.84438(4)	0.0080(2)
W(1)	8*f*	0.27992(7)	0.51275(13)	1.08680(5)	0.0090(2)
W(2)	8*f*	0.08111(7)	0.49831(13)	0.68717(4)	0.0079(2)
O(1)	4*e*	0	0.434(4)	3/4	0.018(5)
O(2)	8*f*	0.2044(12)	0.455(3)	0.7754(7)	0.013(4)
O(3)	8*f*	0.1893(11)	0.564(3)	0.6502(8)	0.015(4)
O(4)	8*f*	0.3020(12)	0.225(2)	0.0980(7)	0.012(3)
O(5)	8*f*	0.3885(13)	0.450(3)	0.9128(8)	0.016(4)
O(6)	8*f*	0.1072(12)	0.202(2)	0.6916(8)	0.015(4)
O(7)	8*f*	−0.0911(13)	0.034(3)	0.6822(9)	0.020(4)
O(8)	8*f*	0.0892(12)	0.786(2)	0.7132(7)	0.014(4)
O(9)	8*f*	−0.0104(12)	0.515(2)	0.6256(9)	0.014(4)
O(10)	8*f*	0.1903(14)	0.524(3)	0.0235(8)	0.020(4)
O(11)	8*f*	0.4841(12)	0.227(2)	0.0182(7)	0.014(4)
O(12)	8*f*	0.2732(13)	0.774(3)	0.1252(8)	0.024(4)
O(13)	8*f*	0.3853(13)	0.582(3)	0.0551(8)	0.022(4)
Li	8*f*	−0.102(4)	0.491(7)	0.560(3)	0.022(10)*

3. Description of the crystal structures and discussion

3.1. $Li_2UO_2(WO_4)_2$

The crystal structure of $Li_2UO_2(WO_4)_2$ is built from an assemblage of WO_6 distorted octahedra and UO_7 pentagonal bipyramids to give a three-dimensional arrangement. The only independent uranium atom is bonded to two symmetrical O(1) atoms at short distances of 1.808(13) Å, forming a nearly linear uranyl UO_2^{2+} ion, 179.1(6)°, which is coordinated by five equatorial oxygen atoms, O(2) in the particular (4*c*) site at 2.445(14) Å and two pairs of symmetrical atoms O(6)–O(6)^{i} and O(6)^{ii}–O(6)^{iii} at 2.317(10) and 2.245(9) Å, respectively, to give a pentagonal bipyramidal environment. The UO_7 bipyramids share the symmetrically opposite O(6)–O(6) equatorial edges, creating infinite $(UO_5)_\infty$ chains running down the

Table 6
Anisotropic displacement parameters of U, W and O in $Li_2(UO_2)_4(WO_4)_4O$ ($Å^2$).

Atom	U_{11}	U_{22}	U_{33}	U_{12}	U_{13}	U_{23}
U(1)	0.0097(6)	0.0056(5)	0.0107(6)	0	0.0021(5)	0
U(2)	0.0082(6)	0.0112(6)	0.0087(6)	−0.0005(5)	0.0001(5)	0.0000(4)
U(3)	0.0091(4)	0.0058(4)	0.0085(4)	0.0002(3)	−0.0004(3)	0.0003(3)
W(1)	0.0101(5)	0.0060(4)	0.0113(5)	0.0004(3)	0.0027(4)	0.0001(3)
W(2)	0.0104(5)	0.0052(4)	0.0087(5)	−0.0006(3)	0.0032(4)	−0.0002(3)
O(1)	0.027(15)	0.007(11)	0.021(14)	0	0.010(11)	0
O(2)	0.004(8)	0.017(8)	0.019(10)	0.001(7)	0.002(8)	−0.008(8)
O(3)	0.009(9)	0.010(8)	0.028(10)	0.001(6)	0.008(8)	0.010(7)
O(4)	0.020(10)	0.005(7)	0.010(8)	0.000(6)	0.000(7)	0.003(6)
O(5)	0.016(10)	0.010(8)	0.019(10)	0.002(7)	−0.006(8)	−0.006(7)
O(6)	0.019(11)	0.010(7)	0.021(9)	−0.007(7)	0.015(8)	−0.006(7)
O(7)	0.010(7)	0.012(8)	0.037(12)	0.001(7)	−0.003(8)	0.002(8)
O(8)	0.023(11)	0.005(7)	0.018(9)	0.002(7)	0.012(8)	0.008(6)
O(9)	0.011(9)	0.015(8)	0.015(9)	0.005(8)	0.000(7)	0.010(7)
O(10)	0.010(8)	0.018(9)	0.034(12)	−0.007(7)	0.005(8)	−0.004(8)
O(11)	0.014(9)	0.016(8)	0.010(8)	−0.002(7)	−0.001(7)	−0.001(7)
O(12)	0.018(11)	0.022(10)	0.034(12)	−0.009(8)	0.010(9)	−0.011(8)
O(13)	0.032(12)	0.016(9)	0.022(10)	0.008(8)	0.011(9)	0.001(8)

Note: The anisotropic displacement factor exponent takes the form $-2\pi^2[h^2a^{*^2}U11 + \cdots + 2hka^*b^*U_{12}]$.

Table 7
Bond distances (Å), Angles (°) and bond valences S_{ij} of metal atoms in $Li_2(UO_2)_4(WO_4)_4O$.

U environment

	d_{U-O}(Å)	s_{ij}		d_{U-O}	s_{ij}
U(1)–O(7)	1.82(4)	1.561	U(3)–O(2)	1.83(4)	1.540
U(1)–O(7)^{i}	1.82(4)	1.561	U(3)–O(5)	1.86(4)	1.439
U(1)–O(8)^{ii}	2.27(2)	0.652	U(3)–O(12)^{ix}	2.14(2)	0.834
U(1)–O(8)^{iii}	2.27(2)	0.652	U(3)–O(4)^{v}	2.28(3)	0.649
U(1)–O(6)^{i}	2.36(3)	0.549	U(3)–O(6)^{viii}	2.34(2)	0.569
U(1)–O(6)	2.36(3)	0.549	U(3)–O(3)^{iv}	2.44(2)	0.478
U(1)–O(1)	2.47(3)	0.446	U(3)–O(8)^{iv}	2.46(3)	0.457
$\sum s_{ij}$		5.970			5.966

	d_{U-O}(Å)	s_{ij}		
U(2)–O(11)^{vi}	1.79(2)	1.644	Uranyl angle (°)	
U(2)–O(11)	1.79(2)	1.644		
U(2)–O(13)	2.23(3)	0.708	O(7)–U(1)–O(7)^{i}	176.8 (9)
U(2)–O(13)^{vi}	2.23(3)	0.708	O(11)^{vi}–U(2)–O(11)	180
U(2)–O(5)^{v}	2.32(4)	0.593	O(2)–U(3)–O(5)	176.7 (7)
U(2)–O(5)^{viii}	2.32(4)	0.593		
$\sum s_{ij}$		5.890		

W environment

	d_{U-O}(Å)	s_{ij}		d_{U-o}	s_{ij}
W(1)–O(10)	1.74(4)	1.631	W(2)–O(9)	1.73(4)	1.676
W(1)–O(13)	1.79(3)	1.436	W(2)–O(3)	1.88(3)	1.114
W(1)–O(4)	1.85(1)	1.205	W(2)–O(8)	1.90(1)	1.047
W(1)–O(12)	1.87(2)	1.145	W(2)–O(6)	1.91(1)	1.047
W(1)–O(3)^{x}	2.10(3)	0.620	W(2)–O(1)	1.98(2)	0.857
W(1)–O(7)^{vii}	2.59(5)	0.164	W(2)–O(2)	2.43 (5)	0.255
$\sum s_{ij}$		6.201			5.996

Li environment

	d_{U-O}(Å)	s_{ij}
Li–O(9)	1.80(6)	0.417
Li–O(10)^{i}	2.08(7)	0.185
Li–O(11)^{xi}	2.14(6)	0.162
Li–O(4)^{xi}	2.18(6)	0.145
Li–O(13)^{xiii}	2.70(5)	0.035
Li–O(12)^{xii}	2.85(6)	0.024
Li–O(11)^{xiv}	2.98(7)	0.017
$\sum s_{ij}$		0.985

Symmetry codes: (i) $-x, y, 1.5 - z$; (ii) $-x, -1 + y, 1.5 - z$; (iii) $x, -1 + y, z$; (iv) $0.5 - x, -0.5 + y, 1.5 - z$; (v) $0.5 - x, 0.5 - y, 1 - z$; (vi) $1 - x, 1 - y, -z$; (vii) $0.5 + x, 0.5 - y, -0.5 + z$; (viii) $0.5 - x, 0.5 + y, 1.5 - z$; (ix) $0.5 - x, 1.5 - y, 1 - z$; (x) $x, 1 - y, -0.5 + z$; (xi) $0.5 - x, 0.5 + y, 0.5 - z$; (xii) $-0.5 + x, 1.5 - y, 0.5 + z$; (xiii) $-x, y, 0.5 - z$; (xiv) $-0.5 + x, 0.5 - y, 0.5 + z$.

Table 8
Observed and calculated X-ray powder diffraction pattern for $Li_2(UO_2)(WO_4)_2$.

$h\,k\,l$	$2\theta_{obs}$	$2\theta_{cal}$	$I(\%)$	$h\,k\,l$	$2\theta_{obs}$	$2\theta_{cal}$	$I(\%)$
1 1 0	13.183	13.137	63	0 6 2	49.314	49.336	10
0 2 0	13.903	13.867	89	4 2 1	49.635	49.653	1
1 1 1	17.770	17.777	2	2 6 1	50.140	50.143	3
0 2 1	18.336	18.327	3	3 1 3	51.036	51.043	3
2 0 0	22.399	22.407	100	0 2 4	51.263	51.268	2
1 3 0	23.750	23.712	19	1 7 0	51.329	51.361	1
0 0 2	24.001	23.982	5	2 4 3	52.125	52.130	2
2 1 1	26.401	26.409	18	4 3 1	52.370	52.336	11
2 2 0	26.449	26.443	6	1 7 1	52.954	52.926	3
1 3 1	26.603	26.619	5	4 2 2	54.351	54.359	17
1 1 2	27.410	27.436	28	4 4 0	54.417	54.434	9
0 2 2	27.808	27.804	43	2 0 4	54.590	54.596	10
0 4 0	27.909	27.934	28	2 6 2	54.826	54.819	13
2 2 1	29.079	29.096	3	3 3 3	55.208	55.214	2
0 4 1	30.453	30.468	3	1 3 4	55.225	55.220	3
2 0 2	33.022	33.049	3	3 5 2	55.818	55.812	4
2 3 1	33.136	33.133	8	4 4 1	55.922	55.939	2
1 3 2	33.949	33.975	7	2 5 3	56.751	56.745	2
3 1 0	34.665	34.625	9	0 4 4	57.445	57.429	9
2 2 2	35.987	35.993	44	1 7 2	57.477	57.444	2
2 4 0	36.071	36.097	19	0 8 0	57.746	57.717	2
1 5 0	36.961	36.955	2	5 1 0	58.578	58.597	2
2 4 1	38.159	38.145	2	0 8 1	59.177	59.168	2
1 5 1	38.941	38.965	2	4 1 3	60.231	60.219	8
0 2 3	39.016	39.042	2	4 4 2	60.300	60.306	2
3 3 0	40.127	40.124	10	4 5 1	60.363	60.359	2
3 1 2	42.530	42.558	12	1 8 1	60.428	60.418	3
2 1 3	43.666	43.692	5	5 2 1	61.490	61.469	2
1 3 3	43.833	43.828	2	2 4 4	62.432	62.427	4
2 5 1	43.843	43.868	2	5 3 0	62.433	62.431	4
0 6 1	44.245	44.248	3	2 8 0	62.679	62.700	5
1 5 2	44.571	44.535	9	3 5 3	62.992	62.996	1
2 2 3	45.469	45.475	1	0 8 2	63.386	63.396	1
4 0 0	45.756	45.725	14	4 3 3	63.988	63.994	4
3 3 2	47.278	47.284 2		2 8 1	64.062	64.083	2
4 1 1	47.972	47.990	9	5 1 2	64.261	64.229	3
4 2 0	48.003	48.010	9	1 7 3	64.550	64.515	2
2 3 3	48.355	48.331	2	3 3 4	65.191	65.196	2
2 6 0	48.500	48.514	3	0 6 4	66.851	66.873	1
0 0 4	49.127	49.096	6	2 1 5	67.800	67.795	2

$a = 7.932\ (1)$ Å, $b = 12.769\ (2)$ Å, $c = 7.417\ (1)$ Å, $F_{20} = 51\ (0.0163; 24)$.

Table 9
Observed and calculated X-ray powder diffraction pattern for $Li_2(UO_2)_4(WO_4)_4O$.

$h\,k\,l$	$2\theta_{obs}$	$2\theta_{cal}$	$I(\%)$	$h\,k\,l$	$2\theta_{obs}$	$2\theta_{cal}$	$I(\%)$
0 0 2	08.040	8.060	16	−1 3 4	46.300	46.293	2
−2 0 2	14.021	14.042	2	−1 1 11	47.079	47.074	3
1 1 0	15.440	15.455	11	−6 0 8	47.320	47.302	13
−1 1 1	15.700	15.721	1	3 3 0	47.455	47.481	2
2 0 21	6.159	16.155	13	3 3 1	47.969	47.949	3
−1 1 2	16.960	16.973	2	−4 2 8	48.410	48.438	1
1 1 2	17.880	17.891	7	−7 1 4	48.621	48.598	4
−1 1 3	18.999	19.021	7	−6 2 3	48.880	48.894	1
2 0 4	22.139	22.130	78	5 1 7	49.170	49.189	1
1 1 4	23.101	23.093	32	−3 3 4	49.400	49.376	12
−3 1 1	23.720	23.729	1	−6 2 4	49.660	49.645	4
−3 1 2	24.261	24.257	4	3 3 3	49.950	49.981	1
3 1 1	24.720	24.734	2	7 1 2	50.200	50.182	1
4 0 0	25.741	25.735	11	1 3 6	50.920	50.943	1
3 1 2	26.200	26.192	4	−4 0 12	52.700	52.684	6
−3 1 4	27.180	27.184	100	−8 0 4	52.940	52.899	5
−1 1 6	28.000	28.003	8	3 3 5	53.380	53.363	8
0 2 0	28.300	28.294	36	2 0 12	53.579	53.548	6
0 2 1	28.600	28.588	1	−6 2 7	53.930	53.955	3
0 2 2	29.460	29.455	2	−5 1 11	54.140	54.170	6
0 2 3	30.879	30.850	1	−7 1 8	54.700	54.722	6
−2 2 1	31.160	31.159	4	−5 3 0	54.800	54.766	6
−2 2 2	31.700	31.702	3	−5 3 3	55.040	55.049	1
−3 1 6	32.020	32.025	2	−6 2 8	56.040	56.017	11
−2 2 3	32.740	32.758	5	−5 3 5	56.920	56.924	1
−2 0 8	33.120	33.105	6	1 1 13	57.639	57.658	1
1 1 7	33.300	33.328	1	0 2 12	58.120	58.099	4
−2 2 4	34.299	34.286	2	0 4 0	58.480	58.473	2
0 2 5	34.960	34.977	1	−3 3 9	59.341	59.324	1
−1 1 8	35.240	35.231	25	0 4 3	59.942	59.940	1
5 1 0	35.400	35.381	22	−8 2 1	60.515	60.533	1
2 2 4	36.220	36.190	17	4 2 10	60.700	60.714	1
3 1 6	36.440	36.422	2	−4 2 12	60.860	60.853	6
0 2 6	37.600	37.582	1	−2 4 3	61.100	61.094	4
−4 2 1	38.399	38.381	4	1 1 14	62.101	62.110	1
−4 2 2	38.620	38.615	7	6 0 10	62.562	62.565	1
−4 2 4	40.401	40.394	1	−8 2 6	62.958	62.980	1
−3 1 9	41.540	41.535	1	5 1 11	63.001	63.024	1
−4 2 5	41.881	41.893	1	−2 4 5	63.318	63.317	1
3 1 8	43.219	43.197	13	4 2 11	64.319	64.338	1
4 2 4	43.670	43.676	1	−5 3 9	64.342	64.352	1
−1 3 2	44.100	44.117	4	−7 3 4	64.959	64.976	1
1 3 2	44.519	44.511	3	7 3 1	65.299	65.309	1
6 0 4	44.860	44.830	5	4 4 1	65.360	65.369	1
2 0 10	45.040	45.049	9	9 1 3	65.501	65.497	1
−3 1 10	45.141	45.114	11	−10 0 4	67.040	67.031	6
−4 2 7	45.960	45.949	1				

$a = 14.026\ (2)$ Å, $b = 6.313\ (1)$ Å, $c = 22.306\ (3)$ Å and $\beta = 98.864\ (8)^\circ$, $F_{20} = 36\ (0.0146; 38)$.

c-axis, Fig. 1a. Such infinite chains were observed in many uranyl oxides, where the chains are connected by various ways, as UVO_5 [34], $USbO_5$ [35], UMo_2O_8 [11], $U_2P_2O_{10}$ [36], and other recently studied compounds like uranyl divanadate, $(UO_2)_2V_2O_7$ [37,38], pentahydrated uranyl orthovanadate $(UO_2)_3(VO_4)_2{\cdot}5H_2O$ [39], $M_6(UO_2)_5(VO_4)_2O_5$ with M = Na, K, Rb [40,41], and $K_2(UO_2)W_2O_8$ [26]. The topological studies of uranyl compounds [42] shows the importance of these $(UO_5)_\infty$ chains in the structure of numerous uranyl compounds. The only independent tungsten atom present a distorted octahedral environment of oxygen atoms, with two particularly short distances, W–O(4) and W–O(5), at 1.743(14) and 1.765(9) Å, three intermediates, W–O(2), W–O(3) and W–O(6) at 1.886(1), 1.964(4) and 2.035(9) Å, respectively, and one longer, W–O(4)^{viii} at 2.242(14) Å. Each WO_6 octahedron shares corners O(2), O(3), O(4) and O(4)^{iv} with four adjacent octahedra to form a perovskite layer WO_4 parallel to (010) plane, Fig. 1b. Thus, the crystal structure of this compound is obtained by the association by edge-sharing of these two entities, infinite WO_4 perovskite layers at $y = \frac{1}{4}$ and $\frac{3}{4}$,

and $(UO_5)_\infty$ uranyl chains, giving a three-dimensional framework and creating mono-dimensional tunnels running along the *c*-axis, Figs. 2a and b. The tunnels contain the Li^+ cations disordered on two crystallographic sites.

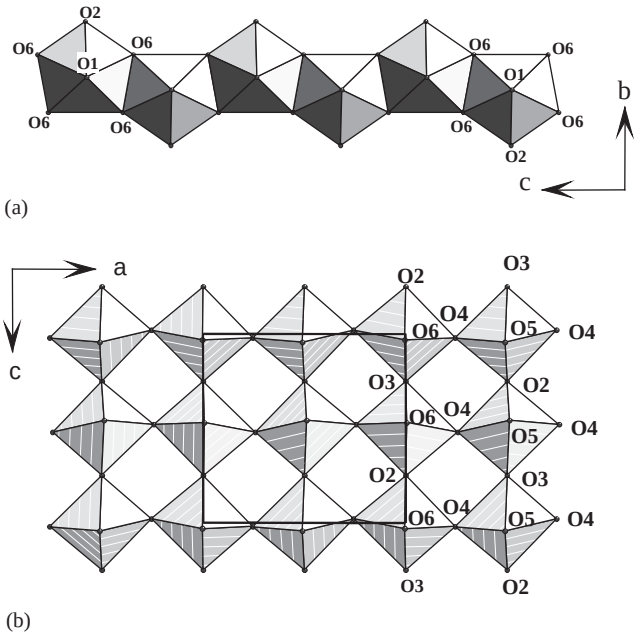

Fig. 1. Representation of the two building entities forming the crystal structure of $Li_2UO_2(WO_4)_2$, (a) $(UO_5)_\infty$ infinite chains of edge-sharing UO_7 pentagonal bipyramids running down the *c*-axis and (b) WO_4 perovskite-type layer of corner-sharing WO_6 octahedra parallel to (010) plane.

Bond valence sums calculation provides values of 6.239, 6.224, 0.751 and 1.044 for U, W, Li(1) and Li(2), respectively, which are consistent with formal valences U^{6+}, W^{6+} and Li^+. For oxygen atoms the calculated valence bond sums ranged from 2.022 to 2.272 with an average value of 2.173, showing that the oxygen atoms are only in the ion oxide form.

The structure of $Li_2UO_2(WO_4)_2$ is different to that of other $M_2UO_2(WO_4)_2$ compounds with M = Ag, Na, K, Rb, recently described [26,27]. In all cases, the structure results from two chains, (i) $(UO_5)_\infty$ infinite chains built from UO_2^{2+} uranyl ion in pentagonal bipyramid coordination shared by equatorial edges and (ii) $(WO_5)_\infty$ chains built from WO_6 octahedra shared by corners. In these last compounds (M = Ag, Na, K, Rb), WO_6 octahedra of two adjacent chains share edges to form $(W_2O_8)_\infty$ double chains. These infinite double chains $(W_2O_8)_\infty$ are also connected to the uranyl $(UO_5)_\infty$ chain by sharing edges to give sheets $[(UO_2)W_2O_8]^{2-}$. The alkaline ions are located in the interlayer spaces between these sheets. While in $Li_2UO_2(WO_4)_2$ compound, infinity of parallel $(WO_5)_\infty$ chains share opposite corners to form parallel perovskite sheets of WO_6 octahedra which are linked together by $(UO_5)_\infty$ uranyl infinite chains to create tunnels populated by the lithium ions. In fact, only Li^+ can be accommodate to the dimensions of the channels, so the ionic radius of the alkaline ion governs the type of structure obtained, open framework or layered network.

It is also interesting to compare the structure of $Li_2UO_2(WO_4)_2$ ($Li_2UW_2O_{10}$) with those of UMO_5 (M = Mo, Sb, V, Nb) compounds which contain

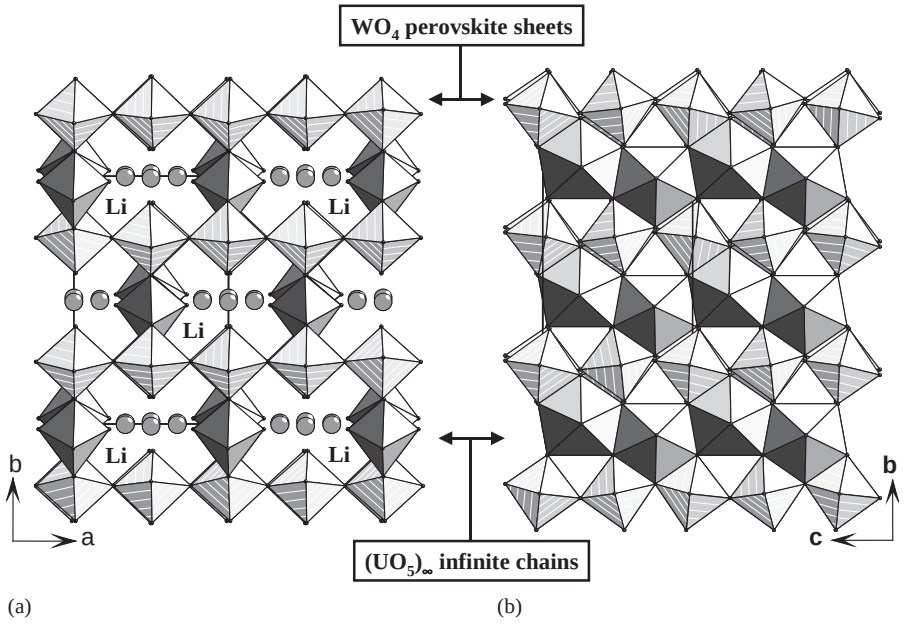

Fig. 2. Projection of the $Li_2UO_2(WO_4)_2$ crystal structure, (a) view on the (001) plane showing WO_4 perovskite layers staked along *b*-axis which are linked by $(UO_5)_\infty$ infinite chains to create tunnels occupied by Li atoms and (b) view of the structure in the (100) plane. Note that two successive $(UO_5)_\infty$ infinite chains are not at the same *x*-coordinate.

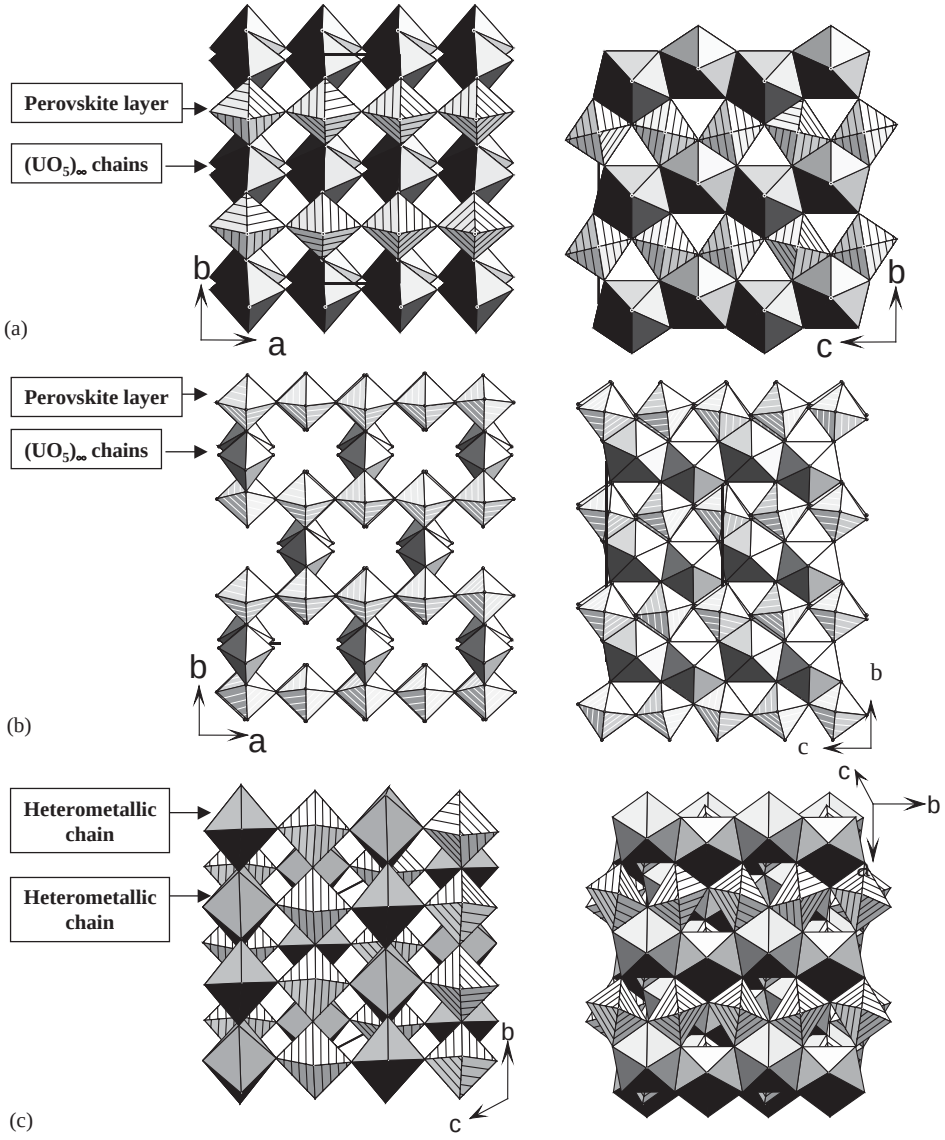

Fig. 3. Crystal structures of compounds built from MO_4 perovskite-type layers connected by $(UO_5)_\infty$ infinite chains, (a) UMO_5 compounds (M = Mo, V, Nb), (b) $Li_2UO_2(WO_4)_2$ where half of the $(UO_5)_\infty$ infinite chains are missing and (c) $USbO_5$ where successive uranophane anion sheets are translated.

U^{4+} (M = Mo) [43] or U^{5+} (M = Sb, V, Nb) [34,35,44]. In these compounds, $(UO_5)_\infty$ chains share edges with square bases of MO_6 distorted octahedra (Fig. 3). The resulting layers, of uranophane sheet anion topology [42] where pentagons are occupied by U and squares by W, are stacked in registry by perpendicular chains containing –U–O–U–O– and –M–O–M–O– for M = Mo, V, Sb leading to the formation of MO_4 perovskite-type slabs. In these compounds, no uranyl group is present, the U–O bond lengths along the chains perpendicular to the layers are greater than 2.0 Å. In $Li_2UO_2(WO_4)_2$ one-half of the U atom are missing, so the layers do not exist any more but the arrangement in a plane is limited to ribbons of one $(UO_5)_\infty$ chain flanked on both sides by chains of WO_5 corner-sharing octahedra, two consecutive ribbons are translated of $(a+b)/2$, so the –M–O–M–O– chains and then the perovskite-type layers remain while the –U–O–U–O– chains are broken and limited to O = U = O entities. One can imagine that half of the U atoms of the UMO_5 structure is removed and substituted by Li allowing the formation of the short uranyl bonds. Surprisingly, $USbO_5$ [35] differs of the other UMO_5 (M = Mo, V, Nb) [34,43,44] compounds in the stacking of the layers, displacement of successive layers leads to heterometallic –U–O–Sb–O–U–O–Sb–O– chains (Fig. 3c). The parameters of the orthorhombic unit cell of UMO_5 (M = Mo, V, Nb) and $Li_2UO_2(WO_4)_2$ are comparable

Table 10
Orthorhombic unit cell parameters and metal-oxygen distances in the –*M*–O–*M*–O– chains for $Li_2UO_2(WO_4)_2$ and UMO_5 (*M* = Mo, V, Nb).

Compound	*A*	*b*	*C*	d_{M-O}	
$Li_2UO_2(WO_4)_2$	7.9372(15)	12.786(2)	7.4249(14)	1.765(9)	2.242(15)
$UMoO_5$	4.1252(2) × 2	12.746(1)	7.3494(7)	1.655(8)	2.471(8)
UVO_5	4.1231(1) × 2	12.3641(1)	7.2071(1)	1.648(5)	2.476(5)
$UNbO_5$	4.124(4) × 2	6.434(4) × 2	7.434(4)	1.700(2)	2.424(2)

and, systematically short and long *M*–O distances alternate in the –*M*–O–*M*–O– chains (Table 10). The existence of a solid solution of the type $Li_{2x}U^{6+}_{x}U^{4+}_{2-2x}M^{6+}_{2}O_{10}$ can thus be imagined with molybdenum or the tungsten; unfortunately, the phase UWO_5 does not exist and $Li_2UO_2(MoO_4)_2$ adopts a completely different structure based on chains of corner-sharing uranyl square bipyramids and MoO_4 tetrahedra [45].

3.2. $Li_2(UO_2)_4(WO_4)_4O$

The crystal structure of $Li_2(UO_2)_4(WO_4)_4O$ contains three independent uranium atoms, U(1) and U(2) in particular positions (4*e*) and (4*a*), respectively, and U(3) in a general (8*f*) site. Each uranium cation is strongly bonded at short distances to two oxygen atoms: O(7) and O(7)^{i} at 1.82(4) Å for U(1); O(11) and O(11)^{vi} at 1.79(2) Å for U(2) and O(2) at 1.83(4) Å, O(5) at 1.86(4) Å for U(3), forming a perfectly linear uranyl ion with U(2) atom and approximately linear uranyl ions with U(1) and U(3), Table 7. The U(1)O_2^{2+} uranyl ion is coordinated by five oxygen atoms, located at the equatorial vertices of a pentagonal bipyramid, with O(1) at 2.47(3) Å, and symmetrically disposed to O(1)–U(1)–O(7) plane, O(8)^{ii}, O(8)^{iii} and O(6), O(6)^{i} at 2.27(2) Å and 2.36(3) Å, respectively. This coordination is also observed for U(3) with equatorial atoms, O(12)^{ix}, O(4)^{v}, O(6)^{viii}, O(3)^{iv}, O(8)^{iv} situated in the range 2.14(2)–2.46(3) Å. The U(2) atom is situated in less common tetragonal bipyramid environment, where the U(2)O_2^{2+} uranyl ion is surrounded in the equatorial plane by diametrically opposed O(13), O(13)^{vi} and O(5)^{v}, O(5)^{viii} atoms at 2.23(3) and 2.32(4) Å, respectively. In this compound, the equatorial mean bond lengths of 2.35(2) and 2.34(2) Å for U(1)O_2^{2+} and U(3)O_2^{2+} in pentagonal bipyramid coordination, and of 2.28(3) Å for U(2)O_2^{2+} uranyl ion in tetragonal bipyramid environment are in excellent agreement with the average bond lengths of 2.37(9) and 2.28(5) Å determined by Burns et al. [31] from numerous well-refined structures, for uranyl ions in pentagonal and tetragonal bipyramid coordination, respectively. There are two independent tungsten sites W(1) and W(2) in the structure of $Li_2(UO_2)_4(WO_4)_4O$. Both W atoms present a strongly distorted octahedral environment of oxygen atoms. The W(2) octahedron is formed in the equatorial plane by O(3), O(8), O(6), O(1)

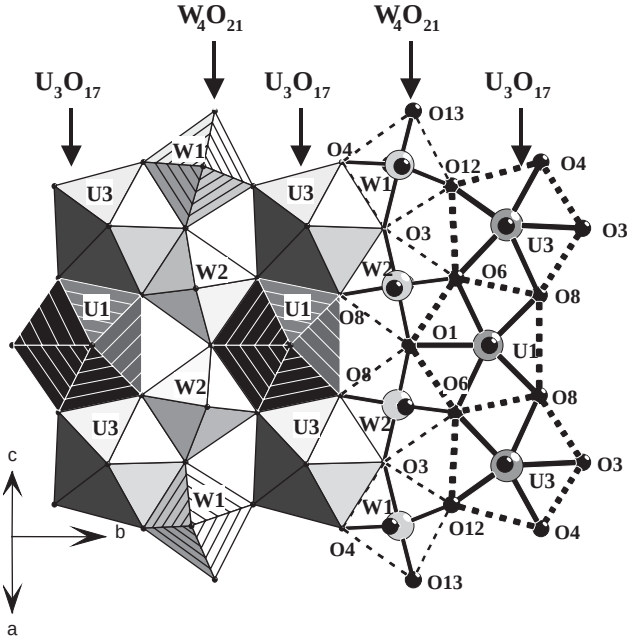

Fig. 4. View on the (102) plane of the tetrameric W_4O_{21} tungstate groups connected to the neighboring trimeric U_3O_{17} uranyl units, to give a $[U_3W_4O_{27}]$ uranyl tungstate ribbon, four octahedra wide.

atoms with distances in the range 1.88(3)–1.98(2) Å and by two apical oxygen atoms O(9) and O(2), which form a short (1.73(4) Å) and a long bond (2.43(5) Å), respectively. For the W(1) octahedron, the oxygen atoms O(13), O(4), O(12) and O(3)^{x}, in the equatorial plane, are in the range 1.79(3)–2.10(3) Å whereas the apical atoms O(10) and O(7) are at 1.74(4) and 2.59(5) Å, respectively. This strong distorted octahedral geometry is observed in other W containing compounds with four intermediate bonds, one short and one long in a *trans* arrangement [26,27].

In the structure of $Li_2(UO_2)_4(WO_4)_4O$, one U(1)O_7 pentagonal bipyramid shares two opposite edges O(6)–O(8) with two adjacent U(3)O_7 bipyramids to form a trimeric unit U_3O_{17}, Fig. 4. The distorted tungsten octahedra are associated in linear sequences W(1)O_6–W(2)O_6–W(2)O_6–W(1)O_6 by sharing opposite corners O(3), O(1), O(3) to give a tetrameric group W_4O_{21}, Figs. 4 and 5. These W_4O_{21} tetrameric units alternate regularly along *b* with trimeric U_3O_{17} units, to whom

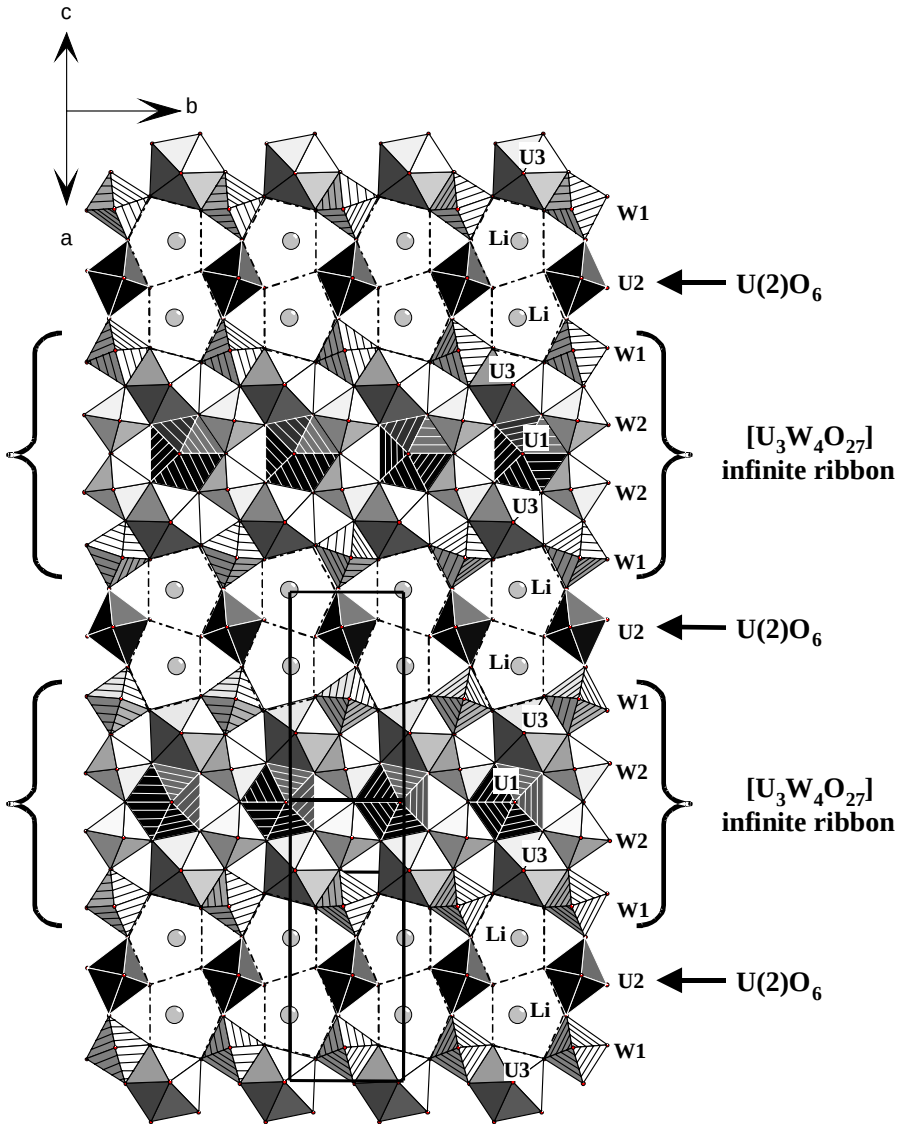

Fig. 5. Projection on the (102) plane of the $[U_4W_4O_{31}]$ layer of the $Li_2(UO_2)_4(WO_4)_4O$ compound resulting from the connection of $[U_3W_4O_{27}]$ ribbons by $U(2)O_6$ octahedra. The pentagonal holes of the polyhedral bi-dimensional arrangement are populated by Li atoms.

they are linked by sharing equatorial edges and corners, to form an infinite $[U_3W_4O_{27}]$ ribbons, four WO_6 octahedra wide, Fig. 4. The uranyl U = O and the short and long W–O bonds are perpendicular to the plane of the ribbon. This ribbon constitutes part of the layer arrangement found, for example, in UMO_5 (M = Mo, Sb, V, Nb) compounds [34,35,43,44].

Two parallel ribbons related by the inversion center occupied by the uranium atom U(2) in special position (4*a*), are linked together by $U(2)O_6$ tetragonal bipyramids sharing opposite equatorial corners O(13) with $W(1)O_6$ octahedra, to form an infinite $[U_4W_4O_{31}]$ layer parallel to (102) plane, Fig. 5. The uranyl bonds U(2) = O(11) are, contrary to other uranyl bonds, in the layer. The layered arrangement of pentagonal bipyramids and octahedra creates holes formed from two edge-shared pentagons flanked by two triangles, Fig. 5. The centers of pentagons are occupied by the Li atoms. The coordination around Li is completed by two oxygen atoms O(9) and O(10) at short distances to form a distorted pentagonal bipyramid. In fact, the Li^+ ion is displaced from the center of the pentagon toward the O(4)–O(11) edge leading to a distorted tetrahedral environment if only the short Li–O distances are considered, Fig. 6. Considering the LiO_7 entities, the bi-dimensional arrangement obtained from UO_7 and LiO_7 pentagonal bipyramids and from WO_6 and UO_6 distorted octahedra, are similar to the common layers observed in the UMO_5 (M = Mo, Sb, V, Nb) compounds [34,35,43,44] and based on the uranophane sheet anion topology [42] shown in Fig. 7; these sheets are built from pentagons whose centers are populated by U

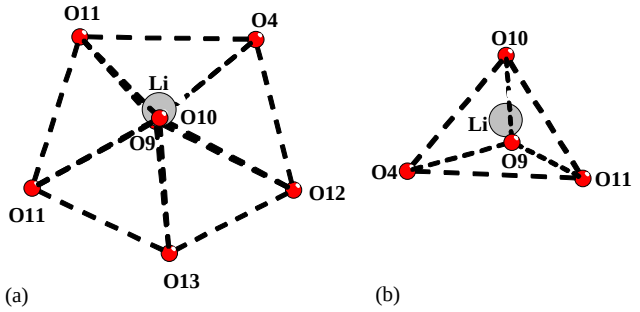

Fig. 6. Environment of the lithium ion in $Li_2(UO_2)_4(WO_4)_4$ from (a) pentagonal bipyramid to (b) distorted tetrahedron.

and Li in an ordered sequence 3U–2Li and form squares whose centers are occupied by U and W in an ordered sequence 1U–4W in such a way that the square whose center is populated by U shares its edges or corners with pentagons whose centers are only occupied by Li. It is the first example of compound with uranophane sheet anion topology with the centers of the squares and pentagons, both populated by U and an other metallic atom. For sheets with occupied triangles as in $Na_{6-x}(UO_2)_3(H_xPO_4)(PO_4)_3$ with $x = 0.5$ [46], the pentagons are half populated by U and Na atoms in pentagonal bipyramid coordination.

The stacking perpendicularly to (102) plane of successive layers deduced one from the other by the $(a+b)/2$ translation, is effectuated by sharing the oxygen atoms that do not participate to the sheet formation leading to perpendicular heterometallic infinite chains –O(5)–U(2)–O(5)–U(3)–O(2)–W(2)–O(9)–Li–O(10)–W(1)–O(7)–U(1)–O(7)–W(1)–O(10)–Li–O(9)–W(2)–O(2)–U(3)–O(5)–U(2)–O(5)–, Fig. 8. Thus, the piling of these layers generates a lithium uranyl tungstate framework $[Li_2U_4W_4O_{25}]$. We can also consider that the uranium and tungsten polyhedra form a new uranyl tungstate framework $[U_4W_4O_{25}]^{2-}$ with rectangular mono-dimensional channels running along the $[\bar{1}10]$ direction with approximate dimensions $2.8\,\text{Å} \times 5.6\,\text{Å}$, which are occupied by lithium cations, Fig. 9.

On the basis of U–O, W–O and Li–O distances, the calculated bond valence sums are 5.97 v.u. for U(1) and U(3), 5.89 v.u. for U(2), 6.20 and 6.00 v.u. for W(1) and W(2), respectively, and 0.985 v.u. for Li, these values are consistent with formal valences of U^{6+}, W^{6+} and Li^+. The bond valence sums for the O atoms are in the range of 1.75–2.17 v.u. with an average value of 2.08 v.u.

To evidence the lithium cations mobility in the tunnels of the two structures, ionic conductivity measurements were carried out. Thus, Fig. 10 indicates the temperature dependence of the conductivity for both compounds. The observed linear evolution of $\log\sigma$ with reverse temperature shows that the ionic conductivity obeys to the Arrhenius law over the studied temperature range,

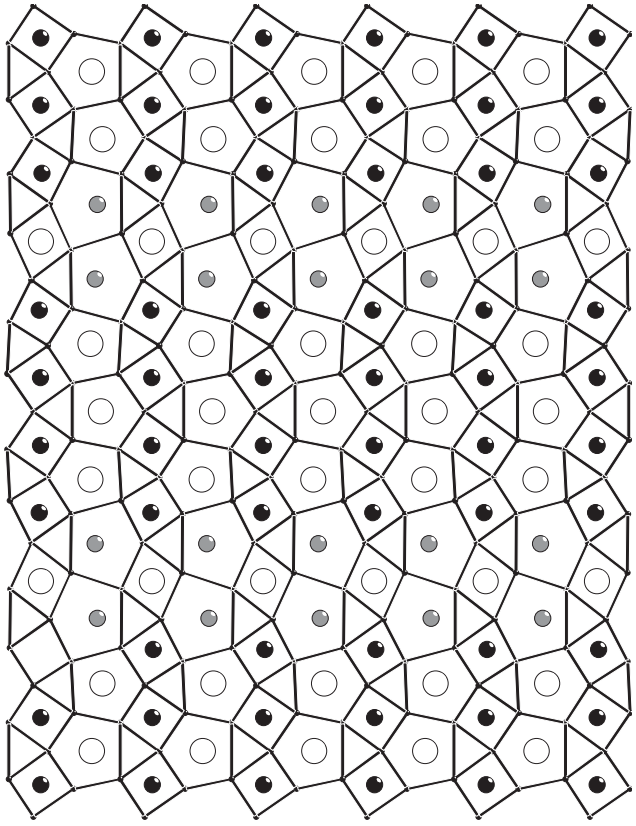

Fig. 7. The uranophane sheet anion topology. In $Li_2(UO_2)_4(WO_4)_4O$ the centers of the pentagons are populated by U and Li in an ordered sequence 3U–2Li and the centers of the squares are occupied by U and W in an ordered sequence 1U–4W.

with activation energy values of 0.71 and 0.81 eV for $Li_2(UO_2)_4(WO_4)_4O$ and $Li_2(UO_2)(WO_4)_2$, respectively. The observed values are comparable to those of the better Li^+ ion conductivity solid electrolytes such as LISICON or Li-β-alumina.

4. Conclusion

In accordance with the numerous previous investigations of the uranyl-containing compounds, this study confirms the complexity and interest of the crystal chemistry of the uranyl tungstates and the key role of the alkali cation on both connectivity and dimensionality of the obtained crystal structures. While Na, K or Rb occupy the inter-space between layers formed by the linkage of uranyl and tungsten polyhedra [26,27], the smaller Li counter-cation leads to the formation of frameworks. It has been shown above that the structures of $Li_2UO_2(WO_4)_2$ and $Li_2(UO_2)_4(WO_4)_4O$ are related to those of UMO_5 ($M = Mo$, Sb, V, Nb) compounds [34,35,43,44]. In $Li_2UO_2(WO_4)_2$, one-half of the $(UO_5)_\infty$

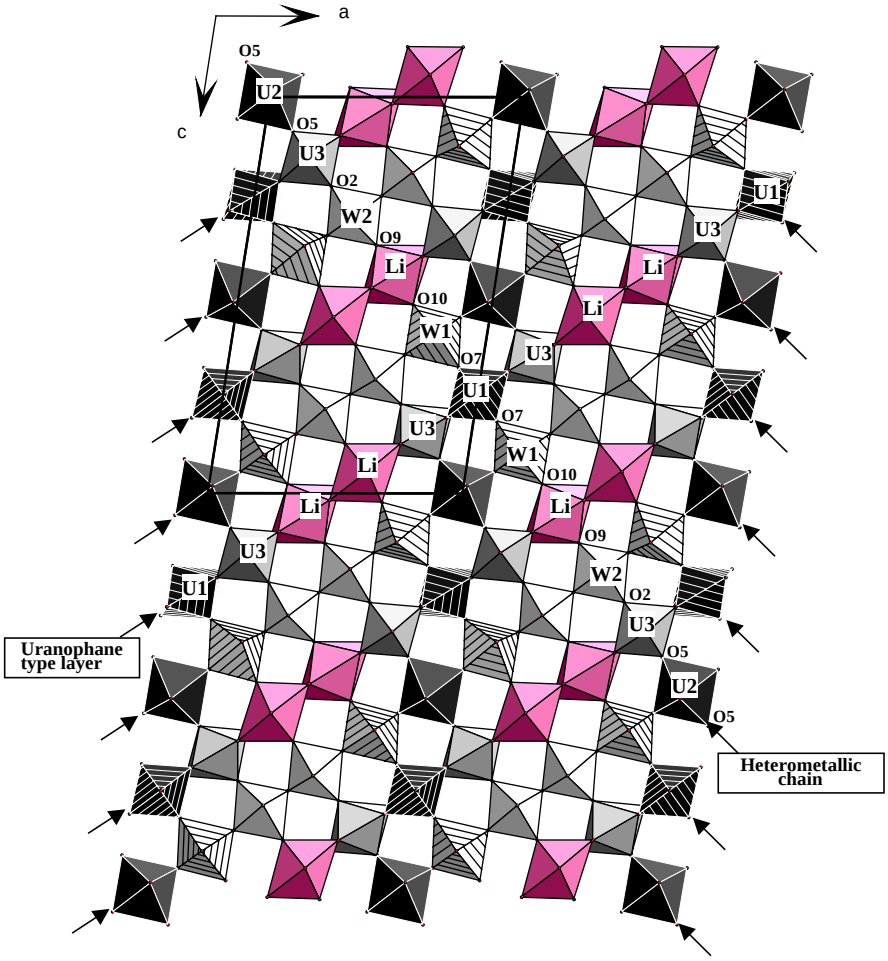

Fig. 8. Stacking of $[Li_2U_4W_4O_{35}]$ layers perpendicular to the (102) plane leading to the formation of heterometallic chains of corner-shared UO_7, UO_6, WO_6 and LiO_7 polyhedra.

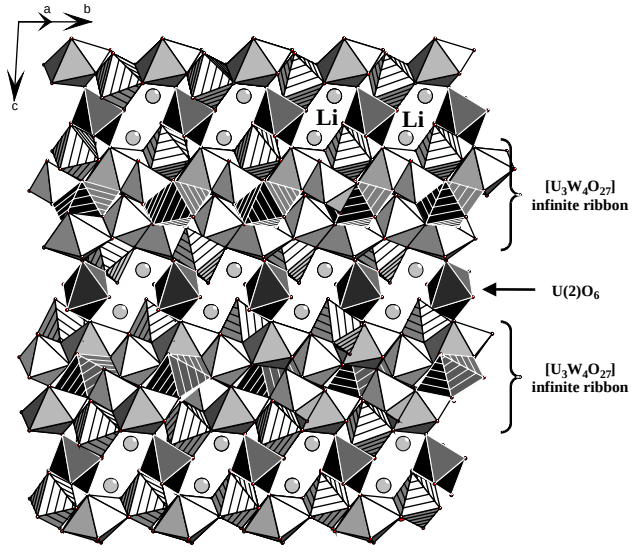

Fig. 9. Projection of the $Li_2(UO_2)_4(WO_4)_4O$ crystal structure on the $(\bar{1}01)$ plane showing the rectangular tunnels occupied by Li atoms.

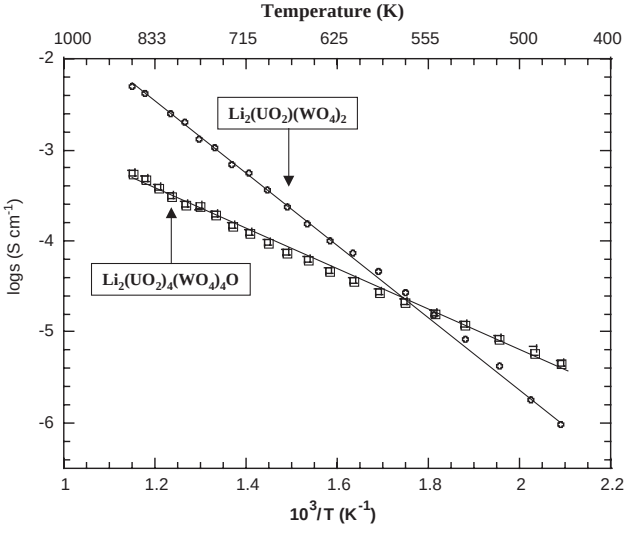

Fig. 10. Temperature dependence of ionic conductivity for $Li_2(UO_2)(WO_4)_2$ and $Li_2(UO_2)_4(WO_4)_4O$ compounds.

chains are missing and replaced by Li cations. In $Li_2(UO_2)_4(WO_4)_4O$ we have demonstrated that LiO_7 pentagonal bipyramids can replace UO_7 bipyramids in the $(UO_5)_\infty$ chains of the uranophane sheet anion topology [42], the connection between polyhedra perpendicularly to the sheet leads to a three-dimensional arrangement as in UMO_5 compounds.

References

[1] S.V. Krivovichev, P.C. Burns, Can. Mineral. 39 (1) (2001) 207.
[2] I. Duribreux, Thesis, UST-Lille, 1997.
[3] S.V. Krivovichev, C.L. Cahill, P.C. Burns, Inorg. Chem. 42 (7) (2003) 2459.
[4] S.V. Krivovichev, C.L. Cahill, P.C. Burns, Inorg. Chem. 41 (1) (2001) 34.
[5] S.V. Krivovichev, R.J. Finch, P.C. Burns, Can. Mineral. 40 (1) (2002) 193.
[6] G.G. Sadikov, T.I. Krasovskaya, Yu.A. Polyakov, V.P. Nikolaev, Izvzst. Akad. Nauk SSSR, Neutrog. Mater. 24 (1) (1988) 109.
[7] E.A. Tatarinova, L.B. Serezkhin, V.N. Serezkhin, Radiokhimiya 33 (3) (1991) 61.
[8] S.V. Krivovichev, P.C. Burns, Can. Mineral. 39 (1) (2001) 197.
[9] S.V. Krivovichev, P.C. Burns, Can. Mineral. 40 (1) (2002) 201.
[10] S. Obbade, C. Dion, M. Saadi, S. Yagoubi, F. Abraham, J. Solid State Chem. 174 (2003) 19.
[11] T.L. Cremers, P.G. Eller, R.A. Penneman, C.C. Heerick, Acta Crystallogr. 39 (1983) 1163.
[12] S.V. Krivovichev, P.C. Burns, Can. Mineral. 38 (2000) 717.
[13] V.N. Serezkhin, V.F. Chuvaev, L.M. Kovba, V.K. Trunov, Dokl. Akad. Nauk. SSSR. 210 (1973) 873.
[14] S.V. Krivovichev, P.C. Burns, Can. Mineral. 38 (2000) 847.
[15] M. Seleborg, Acta. Chem. Scand. 21 (1967) 499.
[16] B.M. Gatehouse, P. Leverett, J. Chem. Soc. A 6 (1968) 1398.
[17] B.M. Gatehouse, P. Leverett, J. Chem. Soc. D 12 (1970) 740.
[18] L.M. Kovba, V.K. Trunov, A.J. Grigorev, Zh. Strukt. Khim. 6 (1965) 919.
[19] V.N. Serezhkin, V.V. Tabachenko, L.B. Serezhkina, Radiokhimiya 20 (1978) 214.
[20] V.N. Serezkhin, L.M. Kovba, V.K. Trunov, Kristallografiya 6 (1972) 1127.
[21] V.N. Serezkhin, L.M. Kovba, L.G. Mokarevitch, Kristallografiya 25 (1980) 858.
[22] M. Sundberg, B.O. Marider, J. Solid State Chem. 121 (1996) 167.
[23] W. Freundlich, M. Pagés, C. R. Acad. Sci. Paris C 269 (1969) 392.
[24] B. Ampe, J.M. Leroy, D. Thomas, G. Tridot, Rev. Chim. Miner. 5 (1968) 789.
[25] A.I. Kryukova, R.A. Bragina, G.N. Kazantsev, I.A. Korshunov, Radiokhimiya 29 (1987) 599.
[26] S. Obbade, C. Dion, E. Bekaert, S. Yagoubi, M. Saadi, F. Abraham, J. Solid State Chem. 172 (2003) 305.
[27] S.V. Krivovichev, P.C. Burns, Solid State Sci. 5 (2003) 373.
[28] G.M. Sheldrick, SAINT Plus version 5.00, Bruker Analytical X-ray Systems, Madison, WI, 1998.
[29] G.M. Sheldrick, "SHELXTL NT, Program Suite for solution and Refinement of Crystal Structure" version 5.1, Bruker Analytical X-ray Systems, Madison, WI, 1998.
[30] G.M. Sheldrick, SADABS: Siemens Area Detector Absorption Correction Program, using SMART CCD based on the method of Blessing: R.H. Blessing; Acta Crystallogr. A 51 (1995) 33.
[31] P.C. Burns, R.C. Ewing, F.C. Hawthorne, Can. Mineral. 35 (1997) 1551.
[32] N.E. Brese, M. O'Keeffe, Acta Crystallogr. B 47 (1991) 192.
[33] G. Smith, R.J. Snyder, J. Appl. Crystallogr. 12 (1979) 60.
[34] P.G. Dickens, C.P. Stuttard, R.G.J. Ball, A.V. Powell, S. Hull, S. Patat, J. Mater. Chem. 2 (1992) 161.
[35] P.G. Dickens, G.P. Stuttard, J. Mater. Chem. 2 (1992) 691.
[36] P. Benard, D. Loüer, N. Dacheux, V. Brandel, M. Genet, Chem. Mater. 6 (1994) 1049.
[37] N. Tancret, S. Obbade, F. Abraham, Eur. J. Solid. State Inorg. Chem. 32 (1995) 195.
[38] A.M. Chippindale, P.G. Dickens, G.J. Flynnand, C.P. Stuttard, J. Mater. Chem. 5 (1995) 141.
[39] M. Saadi, C. Dion, F. Abraham, J. Solid State Chem. 150 (2000) 72.
[40] C. Dion, S. Obbade, E. Raekelboom, F. Abraham, M. Saadi, J. Solid State Chem. 155 (2000) 342.
[41] S. Obbade, M. Saadi, L. Duvieubourg, C. Dion, F. Abraham, J. Solid State Chem. 173 (2003) 1.
[42] P.C. Burns, M.L. Miller, R.C. Ewing, Can. Mineral. 34 (1996) 845.
[43] O.G. D'yachenko, V.V. Tabachenko, R. Tali, L. Kovba, B.O. Marinder, M. Sundberg, Acta Crystallogr. B 52 (1996) 961.
[44] M. Schleifer, J. Busch, R. Gmelin, Z. Anorg. Allg. Chem. 625 (1999) 1985.
[45] V. Krivovichev, P.C. Burns, Solid State Sci. 5 (2003) 481.
[46] Yu.E. Gorbunova, S.A. Linde, A.V. Lavrov, A.B. Pobedina, Dokl. Akad. Nauk SSSR 251 (1980) 385.